JACS
JOURNAL OF THE AMERICAN CHEMICAL SOCIETY
Article
Cite This: J. Am. Chem. Soc. 2019, 141, 17150−17157
pubs.acs.org/JACS

Establishing a Thermodynamic Landscape for the Active Site of Mo-Dependent Nitrogenase

David P. Hickey,[†,∥] Rong Cai,[†,∥] Zhi-Yong Yang,[‡] Katharina Grunau,[§] Oliver Einsle,[*,§] Lance C. Seefeldt,[*,‡] and Shelley D. Minteer[*,†]

[†]Department of Chemistry, University of Utah, Salt Lake City, Utah 84112, United States
[‡]Department of Chemistry and Biochemistry, Utah State University, Logan, Utah 84322, United States
[§]Institut für Biochemie and BIOSS Centre for Biological Signaling Studies, Albert-Ludwigs-Universität Freiburg, 79104 Freiburg, Germany

Supporting Information

ABSTRACT: Nitrogenase enzymes are the only biological catalysts able to convert N_2 to NH_3. Molybdenum-dependent nitrogenase consists of two proteins and three metallocofactors that sequentially shuttle eight electrons between three distinct metallocofactors during the turnover of one molecule of N_2. While the kinetics of isolated nitrogenase has been extensively studied, little is known about the thermodynamics of its cofactors under catalytically relevant conditions. Here, we employ a recently described pyrene-modified linear poly(ethylenimine) hydrogel to immobilize the catalytic protein of nitrogenase onto an electrode surface. The resulting electroenzymatic interface enabled direct measurement of reduction potentials associated with each metallocofactor of the nitrogenase complex, illuminating the role of nitrogenase reductase in altering the potential landscape in the active site of nitrogenase and revealing the endergonic nature of electron-transfer steps associated with the conversion of N_2 to NH_3 under physiological conditions.

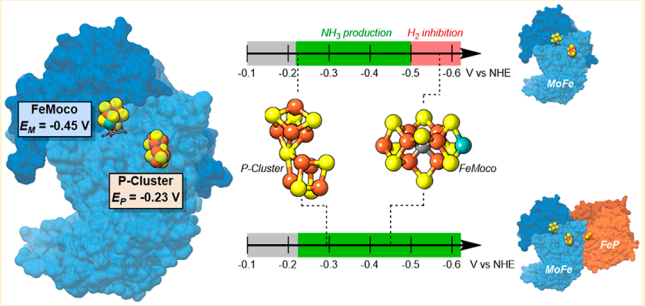

INTRODUCTION

Metalloenzymes have garnered substantial interest due to their ability to catalyze a wide range of challenging reactions ranging from C−H functionalization to N_2 reduction under mild aqueous conditions.[1−5] These enzymes contain a bound metal-ion cofactor whose reactivity is intrinsically tied to the shape of the active site and electronic nature of the metal. Experimentally determined thermodynamic properties of metalloenzymes, such as redox potential, are critical for constructing accurate models of their corresponding active sites and establishing a thorough mechanistic understanding of related biological phenomena. However, characterizing thermodynamic properties of such proteins under non-ground-state conditions remains challenging for techniques that require freeze-quenching because catalytically relevant states are often transient, and for direct electrochemical measurements because the catalytic cofactors are obscured by the protein matrix and not easily accessible to an electrode surface.[6,7] Nitrogenase protein complexes are of substantial environmental interest for their ability to catalyze the reduction of N_2 to NH_3 (Mo-incorporated wild-type)[8,9] as well as CO_2 to various hydrocarbons (V-incorporated variant),[10−12] and they are particularly challenging to study due to the complexity of metallocofactors necessary for catalysis.

The catalytic protein of molybdenum-dependent nitrogenase (MoFe protein) is a dimer of dimers containing a $[Fe_8S_7]$ cluster (P-cluster) and a $[Fe_7MoS_9C]$ cluster (FeMoco).[13−15] The activity of nitrogenase *in vivo* depends on a $[Fe_4S_4]$ cluster-containing nitrogenase reductase (FeP) as a unique electron donor.[16,17] During catalysis, electrons are initially transferred from the P-cluster to FeMoco upon binding of FeP to MoFe via a deficit spending mechanism, in which electrons are subsequently back-filled into the P-cluster from FeP.[18] Once transferred from the P-cluster, electrons are trapped in the form of Fe hydrides around the Fe centers of FeMoco and are subsequently utilized to reduce N_2.[19−23] While the kinetics of MoFe have been extensively studied,[22,24,25] the thermodynamic driving forces that enable its exceptional reactivity remain poorly understood. We recently described a pyrene-modified linear poly(ethylenimine) (pyrene-LPEI) hydrogel capable of establishing a coherent bioelectrochemical interface to drive catalysis of several metalloenzymes without the need for an exogenous electron mediator.[26] Consequently, we considered the possibility of employing this approach to directly measure redox potentials for each of the cofactors in nitrogenase under biologically relevant conditions. Herein, we

Received: June 19, 2019
Published: October 2, 2019

DOI: 10.1021/jacs.9b06546
J. Am. Chem. Soc. 2019, 141, 17150−17157

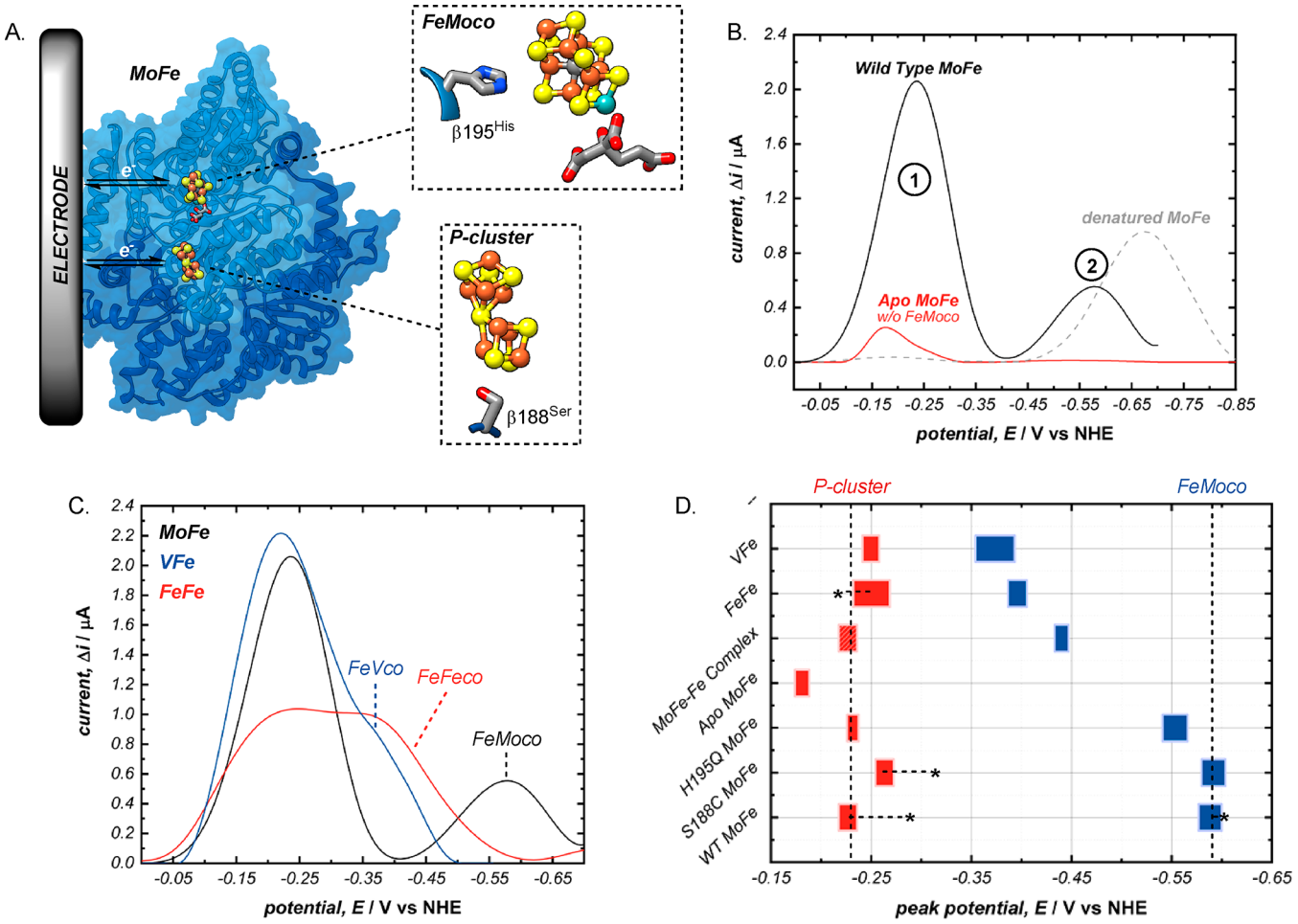

Figure 1. (A) Schematic depicting possible electrochemical interfaces with MoFe protein of the nitrogenase complex, where electron transfer can be measured at either the $[Fe_8S_7]$ (P-cluster) or $[Fe_7MoS_9C]$ (FeMoco) cofactors. (B) Representative SWVs of pyrene-LPEI films containing either wild-type MoFe protein (black line), a MoFe apoprotein (red line) that was expressed without the FeMo-cofactor, or denatured wild-type MoFe protein (dashed line), where **1** is assigned to the P-cluster and **2** is assigned to FeMoco. (C) Representative SWVs of pyrene-LPEI films containing either Mo-nitrogenase MoFe (black line), V-nitrogenase VFe (blue line), or Fe-nitrogenase FeFe (red line), where the corresponding P-cluster remains relatively unchanged and the catalytic cofactor differs by one metal atom. (D) Summary plot of peak potentials for the P-cluster and FeMoco (or catalytic equivalent) clusters corresponding to several variants of the MoFe protein, where the horizontal bars represent one standard deviation around the mean value with $n = 3$, and * represents analogous literature values as detailed in the Supporting Information. All SWVs were performed at 30 Hz with an amplitude of 20 mV using 100 mM MOPS buffer, pH 7.0, and 25 °C.

utilize electroanalytical techniques to construct a thermodynamic profile of the nitrogenase complex. Furthermore, recent studies have demonstrated the use of photochemistry or electrochemistry to drive the catalytic turnover of the MoFe protein.[27−32] We aim to uncover common mechanistic features of the FeP-driven and electrochemically driven turnover of MoFe during N_2 reduction that may enable the design of novel catalytic motifs.

RESULTS

Redox Potential of Nitrogenase Cofactors. To initiate our investigation, we aimed to determine the reduction potential of the relevant cofactors of nitrogenase under non-turnover conditions. Therefore, immobilization of MoFe in the absence of FeP would enable measurement of cofactors in the absence of background catalysis. Due to the likely low concentration of properly oriented protein to enable electrochemical communication, we employed square wave voltammetry (SWV) as a highly sensitive electrochemical technique (full discussion of optimization is provided in the Supporting Information, Figures S1−S3). SWV of pyrene-LPEI films containing wild-type MoFe under an atmosphere of Ar with 3% H_2 (Figure 1) revealed two distinct redox features at −0.23 ± 0.01 V (**1**) and −0.59 ± 0.01 V (**2**) (all potentials are reported vs NHE). These potentials are consistent with previously reported values for the resting/singly oxidized P-cluster redox couple ($P^{N/+}$; −0.30 V at pH 7.5)[33] and the resting/reduced redox couple of the isolated FeMoco ($M^{N/R}$; −0.60 V),[34] respectively (while the only reported value for active FeMoco was estimated using kinetic analysis to be −0.48 V under pure Ar at pH 8).[35] In order to more precisely assign each peak, we compared SWVs of wild-type MoFe with that of an apo mutant that does not contain the catalytically active FeMoco cluster,[36,37] as well as V-nitrogenase and Fe-nitrogenase (where the molybdenum atom of FeMoco is replaced by vanadium or iron, respectively).[38,39] While **1** remains virtually unchanged for each nitrogenase isozyme, the resulting voltammograms (Figure 1) reveal a dramatically different potential of **2** for V-nitrogenase (−0.38 ± 0.02 V) and

DOI: 10.1021/jacs.9b06546
J. Am. Chem. Soc. 2019, 141, 17150−17157

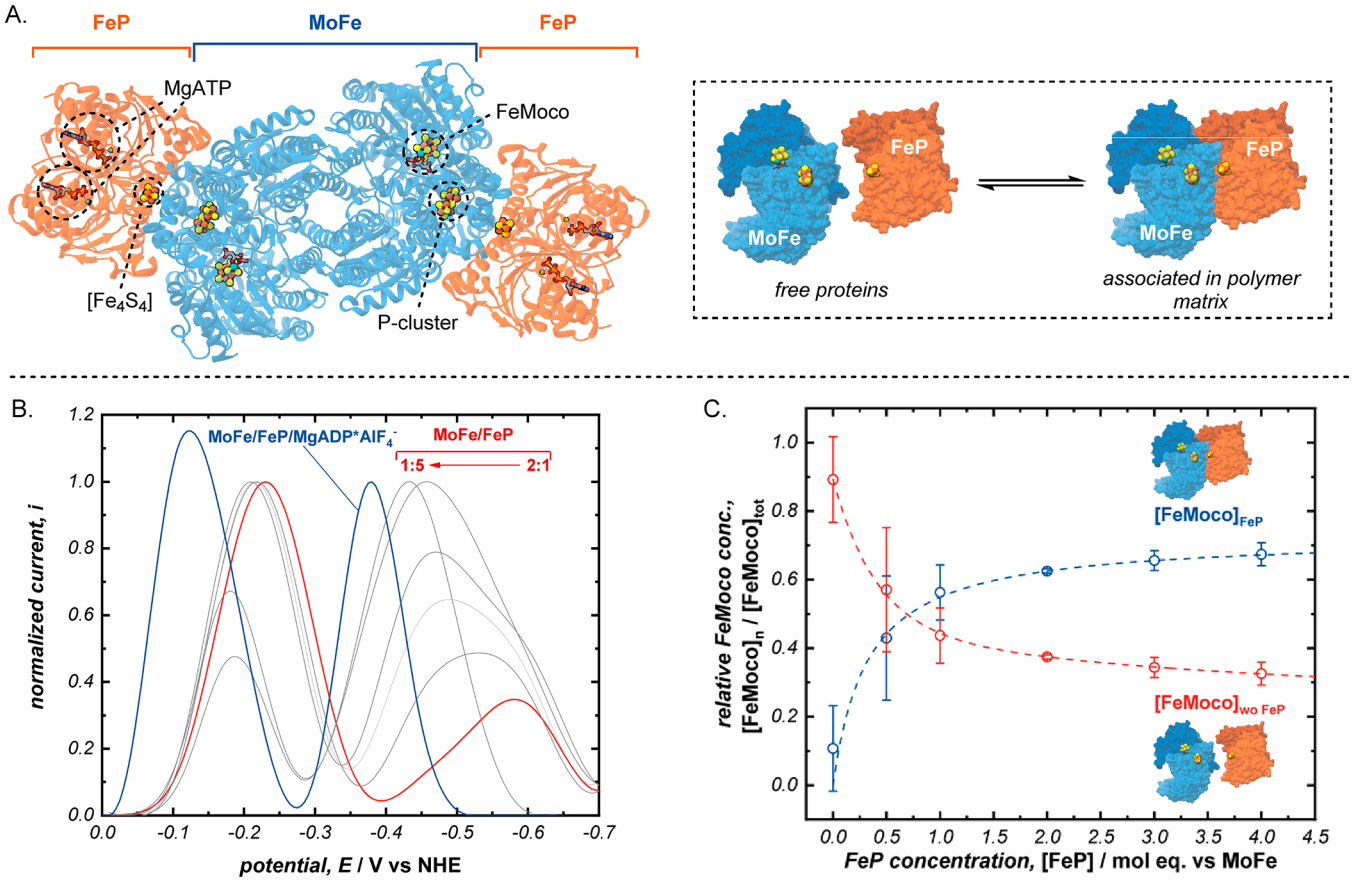

Figure 2. (A) Scheme of the nitrogenase complex consisting of the Fe-protein (FeP, orange) and the MoFe protein (blue), highlighting the corresponding metallocofactors, and scheme illustrating the association of FeP and MoFe. (B) Representative SWVs of pyrene-LPEI films coated with MoFe and increasing relative concentrations of FeP (0.5, 1, 2, 3, 4, or 5 mol equivalents, red line), or the purified AlF_4^--stabilized MoFe/FeP/MgADP complex (blue line), highlighting the difference in potential of FeMoco upon binding of FeP to MoFe. (C) Binding curve of MoFe in the presence of FeP determined as a function of SWV peak currents. SWVs were performed at 30 Hz with an amplitude of 20 mV under an atmosphere of Ar/H_2 (3.2%) using 100 mM MOPS buffer, pH 7.0, and 25 °C.

Fe-nitrogenase (−0.40 ± 0.01 V),[40−42] and the complete loss of **2** for the apo MoFe version.

It should be noted that the peak currents varied significantly for the same cofactor between different proteins; this is most likely the result of variable concentration of stock protein solution used to prepare electrode films. Furthermore, the small relative peak current observed for the P-cluster of Fe-nitrogenase may be accounted for by difference in the protein's tertiary structure compared to Mo-nitrogenase. Fe-nitrogenase exists as an $\alpha 2\beta 2\delta 2$ heterohexamer, while Mo-nitrogenase is an $\alpha 2\beta 2$ heterotetramer. The difference in tertiary structure may significantly alter the accessibility of the P-cluster in Fe-nitrogenase to the electrode surface, so that fewer immobilized Fe-nitrogenase proteins are oriented to enable electrochemical communication via the P-cluster. While this may provide a rationale for the observed difference in peak height, it is difficult to validate such an argument because a crystal structure for Fe-nitrogenase does not exist as of the writing of this work. Furthermore, this does not account for the fact that V-nitrogenase also exists as an $\alpha 2\beta 2\delta 2$ heterohexamer but exhibits a slightly larger peak current for the P-cluster than Mo-nitrogenase and further studies are needed to address this observation. These results collectively suggest that **2** corresponds to the FeMoco cluster, while a process of elimination would dictate that **1** likely corresponds to the P-cluster.

Because electrochemical measurements cannot, in isolation, be used to correlate a single cofactor within a complex metalloenzyme to a specific peak potential, it is critical to compare a variety of isoforms for a single protein as a method for ensuring correct peak assignment. To this end, comparative SWV was performed on two MoFe proteins with amino acid substitutions (Figure S5), in which the serine-188 residue ligating the P-cluster was replaced with cysteine (S188C)[43] or the histidine-195 residue that acts as a H-bond donor to FeMoco was replaced with glutamine (H195Q).[44] As expected for S188C, the peak corresponding to FeMoco (**2**) remains unchanged, while **1** of S188C is ∼40 mV more reducing (−0.27 ± 0.01 V) than that of wild-type MoFe.[43] For the H195Q mutant, **1** was identical to that of wild-type MoFe, while **2** was shifted to be less reducing (−0.56 ± 0.01 V). Taken together, this evidence is consistent with **1** and **2** arising from electrochemical reduction of the P-cluster ($P^{N/ox}$ couple) and FeMoco ($M^{N/R}$ couple), respectively. A compiled list of potentials is provided in the Table S1.

The general flow of electrons in the MoFe protein has long been suggested to proceed from the P-cluster to the catalytically active FeMoco;[8,19,45] however, our initial voltammetry of MoFe suggests the FeMoco is substantially more reducing than the P-cluster ($E_M - E_P = -0.36$ V), so that there is not sufficient thermodynamic driving force to facilitate electron transfer in this way on a catalytically relevant time

DOI: 10.1021/jacs.9b06546
J. Am. Chem. Soc. 2019, 141, 17150−17157

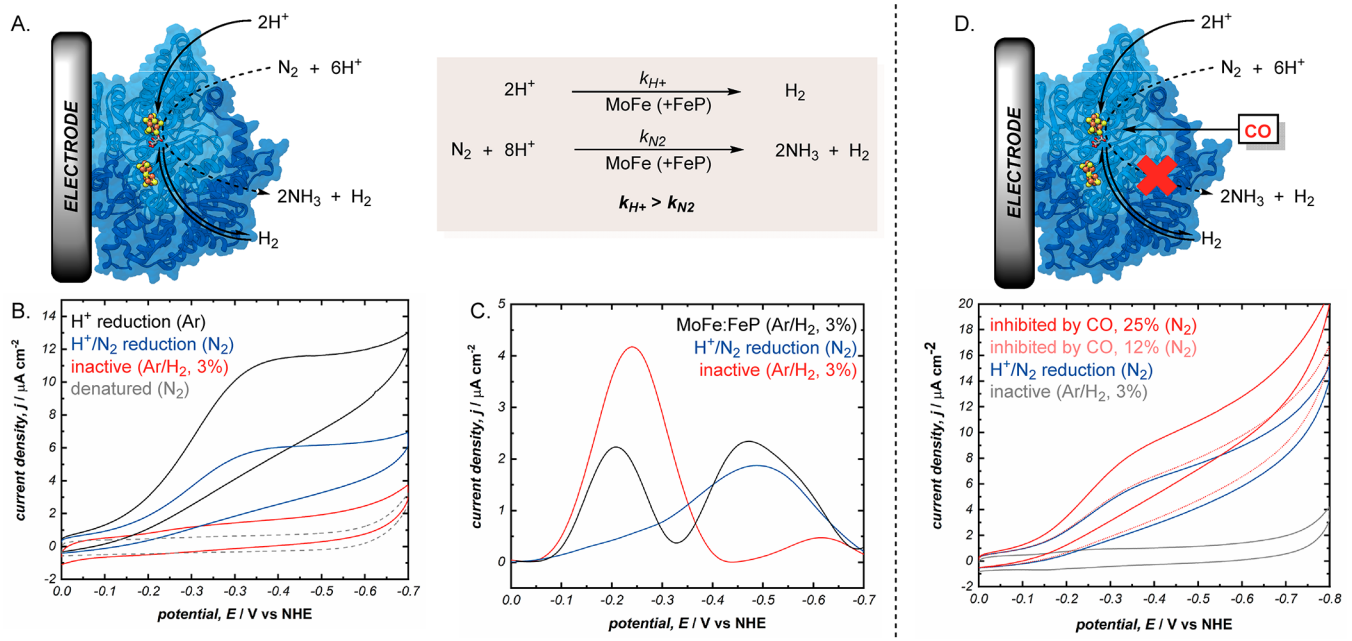

Figure 3. (A) Schematic of possible reactivity of electrochemically interfaced MoFe protein. (B) Representative CVs of pyrene-LPEI/MoFe films under pure Ar (black line), Ar with 3% H_2 (red line), and pure N_2 with active (blue line) or denatured MoFe (dashed line). (C) Representative SWVs of pyrene-LPEI/MoFe films either with (black line) or without (red line) FeP under Ar/H_2, or MoFe under N_2 (blue line). (D) Representative CVs of pyrene-LPEI/MoFe films under Ar/H_2 (black lines), pure N_2 (blue lines), and N_2 with 12% CO (red dotted line) or 25% CO (red solid line). Experiments were performed using 100 mM MOPS buffer, pH 7.0, and 25 °C; CVs were run at 5 mV s^{-1}, and SWVs at 30 Hz with an amplitude of 20 mV.

scale while presuming an electron transfer distance of 14 Å.[46] As a critical component of the *in vivo* catalytic cycle of nitrogenase, FeP transiently associates with MoFe to act as a unique electron donor in the nitrogenase complex.[16] This process requires two equivalents of magnesium adenosine triphosphate (MgATP) per electron transfer for the physiologically relevant $[Fe_4S_4]^{2+/+}$ couple of FeP to MoFe, where it has been proposed that MgATP hydrolysis is necessary to supply the energy required for dissociation of oxidized FeP from MoFe.[47−49] Additionally, binding of FeP to MoFe has been implicated in altering the energetics of electron transfer between the P-cluster and FeMoco;[50,51] specifically, the energy of MgATP and FeP binding is used to alter P-cluster potential.[52] Consequently, we aimed to determine the impact of FeP binding on the redox landscape of FeMoco in the MoFe protein.

Pyrene-LPEI films were prepared with MoFe and varying amounts of FeP. Examining SWVs of the resulting films reveals several noteworthy features (Figure 2). First, when immobilized with relatively low concentration of FeP, MoFe exhibits peaks corresponding to the P-cluster and FeMoco as described above; however, as the relative amount of co-immobilized FeP is increased, a new discrete peak (−0.43 ± 0.02 V) develops with a concomitant decrease in the FeP-absent FeMoco peak (−0.60 ± 0.01 V). In addition, the peak current corresponding to P-cluster decreases relative to that of FeMoco with increasing FeP concentration. The latter observation can be accounted for by the way that FeP binds to MoFe. In the native nitrogenase complex, FeP binding is specific and occurs at the MoFe surface nearest the P-cluster so that the electrochemical accessibility to the P-cluster is dramatically diminished, while that of FeMoco is relatively unaltered. It should be noted here that immobilization of MoFe with denatured FeP does not result in a similar shift in the potential associated with the FeMoco, suggesting that these modulations in potential and peak current arise from protein that has retained some of its native conformation (a detailed explanation of these observations is provided in the Supporting Information, Figure S8). This data suggests that the binding of FeP induces a moderate shift in the reduction potential of FeMoco even in the absence of MgATP. It should be noted that binding of FeP to MoFe in the absence of nucleotides is reported to be very weak, and there are multiple possible binding conformations of MoFe and FeP in the absence of nucleotide.

To provide evidence that the MoFe/FeP complex formed upon immobilization is in a biologically relevant conformation, we employed a MoFe/FeP complex with the tetrafluoroaluminate salt of magnesium adenosine diphosphate (MgADP*AlF_4^-). This complex has previously been reported as an isolatable form of nitrogenase that is stable to dissociation of FeP and not catalytically active. Upon preparing and isolating the MoFe/FeP/MgADP*AlF_4^- complex (full details provided in the Supporting Information), we immobilized it using pyrene-LPEI onto a carbon electrode. Subsequent SWVs revealed a peak redox potential for FeMoco (−0.39 ± 0.03 V) that is in reasonable agreement with that observed for the nucleotide-free MoFe/FeP that was prepared by immobilizing a homogeneously dissolved mixture of MoFe and FeP. These results suggest that either (1) the potential of FeMoco is altered to some extent by binding of FeP in several different conformations, or (2) the local environment created upon immobilization of MoFe and FeP preferentially results in an excess of MoFe/FeP complex bound in its native conformation. At this time, we are unable to distinguish between these possibilities, but both are consistent with an altered reduction potential exhibited by FeMoco upon binding of FeP.

DOI: 10.1021/jacs.9b06546
J. Am. Chem. Soc. 2019, 141, 17150−17157

It might be suggested that the appearance of new peaks in MoFe films prepared with excess equivalents of FeP could be the result of redox activity associated with FeP itself. Multiple attempts were made to immobilize FeP independently and characterize redox couples associate with its [Fe_4S_4] cofactor. However, no consistent peaks were observed under the variety of conditions attempted. It is possible that the cationic environment created by the pyrene-LPEI matrix upon immobilization prevents a coherent interface from being established between the cofactor of FeP and electrode surface. Nevertheless, films prepared using the MoFe/FeP/MgADP*AlF_4^- complex were absent of any excess free FeP and still resulted in an altered FeMoco potential. Finally, an additional peak is observed in films prepared with either MoFe/FeP or the MoFe/FeP/MgADP*AlF_4^- complex that appear at −0.19 ± 0.01 V. The precise identity of this peak is unclear; it may correspond to the oxidized form of FeMoco ($M^{+/2+}$), though precisely equal peak heights would be expected if this were the case (which is not the case for most of the data collected here).

Electrochemically Driven MoFe Catalysis. Provided that this shift in reduction potential is a prerequisite for catalysis, its function remains a significant question. Previous work has demonstrated that H_2 behaves as an inhibitor to N_2 reduction at relatively high concentrations (~10%).[53−56] Consequently, we considered the possibility that H_2 inhibition may be more pronounced in the absence of FeP, so that minimal catalytic activity would be observed in FeP-free systems in the presence of small amounts of H_2. Based on this hypothesis, we studied films containing MoFe without FeP by slow scan rate cyclic voltammetry (CV) under an atmosphere of either Ar/H_2 (3.2%), pure Ar, or pure N_2 (Figure 3). As previously observed in the presence of H_2 (Ar/H_2), MoFe exhibited a small quasireversible redox wave consistent with the P-cluster and no catalytic current. However, under pure Ar, MoFe films exhibited catalytic currents similar to that of MoFe/FeP/MgATP films under Ar/H_2 (data and further description provided in the Supporting Information). Under N_2, a slightly smaller catalytic current density is observed than under pure Ar. This finding would suggest that some aspect of substrate reduction has become a rate limiting step, with the reduction of the more difficult N_2 expected to show a slower rate of electron flow. It is known that with Fe protein as the reductant, a step in the Fe protein cycle is rate limiting, and thus no change in the rate constant of electron flow is seen under different substrates.[52] Furthermore, SWV analysis of MoFe under pure Ar reveals a shift in reduction potential of FeMoco consistent with the shift observed upon the association of FeP in the presence of H_2. Finally, Mo-dependent nitrogenase is known to be reversibly inhibited by CO so that N_2 reduction is prevented without impacting the ability of MoFe to catalyze H^+ reduction.[57,58] To confirm that the differences in current were the result of electrochemically driven MoFe turnover, we measured catalytic current density (j_{max}) by the CV of MoFe in the presence of N_2 with sequentially increasing amounts of CO gas (Figure 3). While intuition would suggest that introduction of CO would lead to a decrease in j_{max} for most heterogeneous electrocatalysts (due to catalyst poisoning, etc.), increasing the partial pressure of CO results in increased values of j_{max} that approach those corresponding to H^+ reduction (observed under pure Ar). Taken together, these data suggest that the electrochemically driven MoFe system exhibits analogous kinetics to the native nitrogenase, H_2 negatively affects the thermodynamic landscape of FeMoco to inhibit catalytic turnover, and binding of FeP mitigates H_2 inhibition of MoFe.

It should be noted that the catalytic current observed via CV under N_2 in the absence of FeP begins at a potential consistent with the P-cluster. While the native electron transport pathway in nitrogenase proceeds through the P-cluster, there have been mixed reports in the ATP-free electrochemically driven nitrogenase system whether electron transport occurs through the P-cluster or directly to the catalytically active FeMoco depending on whether a mediated or direct electrochemical approach was employed.[26,29] Therefore, it became imperative to confirm that the catalytic current observed at the P-cluster corresponds to the enzymatic reduction of N_2 to NH_3.

To accomplish this, we performed bulk electrolysis using MoFe-immobilized films under an atmosphere of pure N_2 under a variety of applied potentials (experimental setup provided in the Supporting Information, Figure S4). Fluorimetric quantification of NH_3 (Figure 4) revealed that

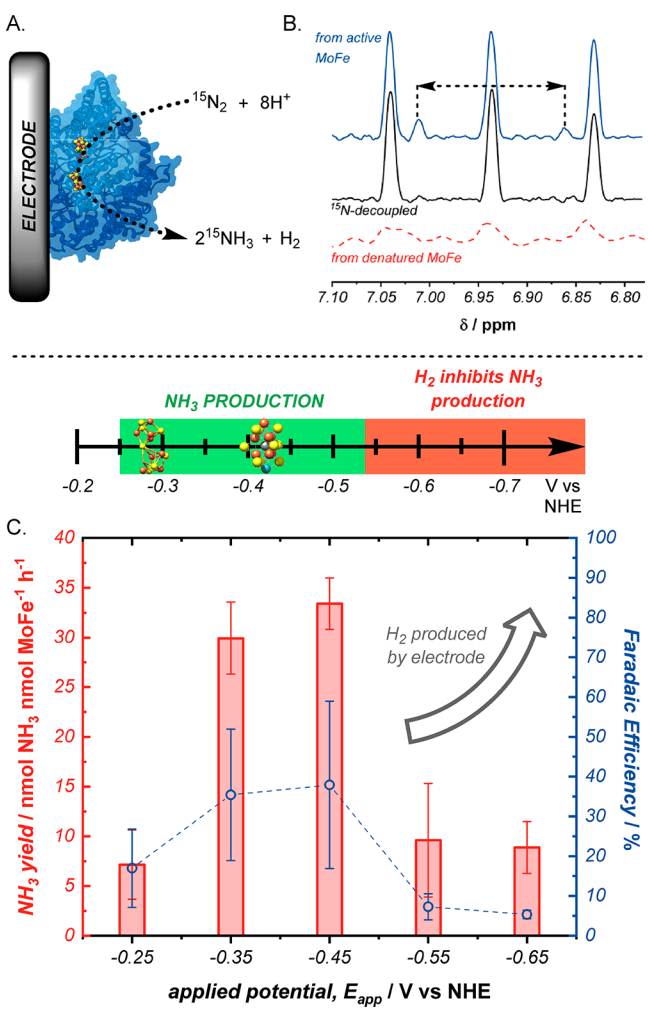

Figure 4. (A) Scheme of electrochemically driven MoFe turnover for $^{15}N_2$ to $^{15}NH_3$. (B) ^{15}N-non-decoupled (blue line) and ^{15}N-decoupled (black line) ^{1}H NMR of $^{15}NH_3$ produced from bulk electrolysis of $^{15}N_2$ using pyrene-LPEI/MoFe electrodes at −0.25 V for 8 h. (B) Amount of ammonia produced (red bars) and Faradaic efficiency (dashed line) for NH_3 production from bulk electrolysis of N_2 using pyrene-LPEI/MoFe electrodes at varying applied potential. Experiments were performed using 50 mM MOPS buffer, pH 7.0, and 25 °C.

DOI: 10.1021/jacs.9b06546
J. Am. Chem. Soc. 2019, 141, 17150−17157

maximum yield and Faradaic efficiency were achieved with an applied potential of −0.45 V; however, NH_3 production was achieved at potentials as high as −0.25 V. Furthermore, a substantial decrease in NH_3 production was observed at applied potentials lower than −0.5 V. This result runs counter to standard intuition according to Butler−Volmer kinetics, which dictates that a stronger reducing potential should provide a greater electrocatalytic driving force outside of the inverted Marcus region. While lower potential may afford a stronger driving force for the electroenzymatic reaction, such low potentials are sufficient to facilitate electrochemical reduction of H^+ by the carbon electrode surface to form H_2 (supported visually by the formation of bubbles on the working electrode). The combination of decreased NH_3 yield and Faradaic efficiency at sufficiently low potentials for H^+ reduction then suggest that a high localized H_2 concentration near the electrode surface may be inhibiting electroenzymatic activity.

In order to confirm that the NH_3 generated was in fact from electroenzymatic turnover of N_2 gas, bulk electrolysis was performed on MoFe-immobilized films under isotopically enriched $^{15}N_2$ at a constant potential of −0.35 V. The electrolysis solution was studied by ^1H NMR with and without ^{15}N decoupling. The resulting NMR spectra revealed a doublet centered around 6.95 ppm with a coupling constant (74 Hz) consistent with $^{15}NH_3$ that, upon ^{15}N decoupling, converged to a singlet. Furthermore, similar electrolysis of $^{14}N_2$ were performed using active and denatured MoFe, and the spectrum resulting from electrolysis with active MoFe reveal a triplet consistent with $^{14}NH_3$ while that of denatured MoFe resulted in no peak formation. It should be noted that a background ammonia signal was observed under all electrochemical conditions using active MoFe films. No such peak was observed when MoFe was denatured prior to immobilization (either under $^{14}N_2$ or $^{15}N_2$), suggesting that the background ammonia signal is being generated from a non-N_2 substrate (Figure S7). Collectively, this data confirms that $^{15}NH_3$ was produced as a result of electrochemically driven MoFe reduction of N_2.

Electron Transfer as a Function of Reduction Potential. Combined with assignment of redox potentials to each metallocofactor, the production of NH_3 at −0.25 V suggests that, similar to the native nitrogenase complex, the electrochemically driven MoFe system proceeds via electron transfer through the P-cluster. Assuming that catalysis occurs at FeMoco in the electrochemical system, this would imply that electron transfer from the less reducing P-cluster to the more reducing FeMoco is a thermodynamically uphill process and thus requires a coupled chemical step to trap the high-energy intermediate. The catalytic cycle of nitrogenase was previously established to proceed via a series of consecutive concerted proton−electron transfers, where an endergonic electron-transfer sequence could conceivably be driven by the formation of Fe-hydride bonds on FeMoco.[8] In order to lend evidence that electrochemically driven MoFe operates by a similar mechanism, the redox potential of the P-cluster was measured under a variety of different pHs ranging from pH = 6.0 to pH = 9.0. The resulting plot of pH versus the peak P-cluster potential, E_p (Figure 5), indicates that the P-cluster potential shifts by ∼41 mV per unit pH. While this is slightly lower than the previously reported change of 53 mV for the $P^{+/2+}$ couple,[18] the discrepancy may be accounted for by the self-buffering nature of the polymer matrix which would dampen

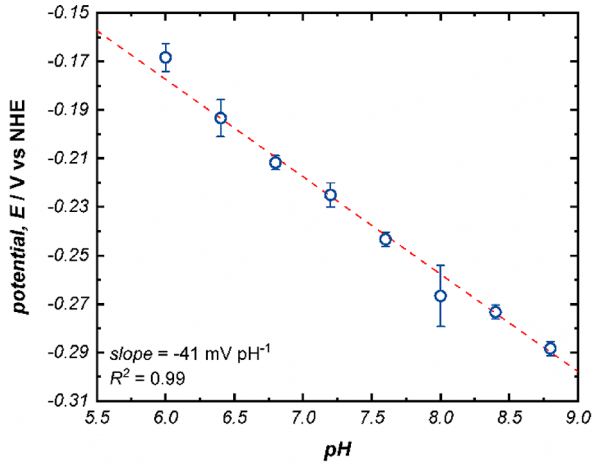

Figure 5. Effect of pH on the peak potential of P-cluster in pyrene-LPEI/MoFe electrode films.

changes in bulk pH.[59] Consequently, this provides evidence that, similar to the native nitrogenase mechanism, electrochemically driven MoFe turnover feasibly occurs via sequential proton-coupled electron-transfer (PCET) steps.[60]

Finally, based on the experimentally measured potentials for P-cluster and FeMoco here, it would seem that endergonic electron-transfer steps are required to drive catalytic turnover of nitrogenase. From the SWV analysis above, H_2-inhibition only impacts the redox potential of FeMoco, so that $\Delta E = E_{FeMoco} - E_{P\text{-cluster}} = -0.43$ and −0.23 V for MoFe under H_2 (3%) and under pure Ar, respectively. However, this does not account for the impact of FeP binding on the potential of the P-cluster. As discussed above, the redox potential of FeMoco was measured in the presence of FeP to better understand the impact of FeP on potential, but the potential of FeP-bound P-cluster was not observed due to steric constraints. Nevertheless, previous studies of FeP-MoFe binding demonstrated that the redox potential of the P-cluster decreases modestly by ∼0.08 V (in the presence of MgATP, determined by EPR redox titration).[61] Combining the shifts in FeMoco reported here with the previously reported shift in P-cluster upon binding of FeP, the driving force from redox potential alone can be described as $\Delta E = -0.12$ V. This data provides experimental justification for endergonic electron transfer in the MoFe protein during the conversion of N_2 to ammonia under both physiological conditions (in the presence of FeP/MgATP) and electrochemical/photochemical conditions (in the absence of FeP). One caveat to this assertion is that measurements cannot exclude any possibility of transient high-energy intermediates that may exist, and more work is needed to probe for such species.

CONCLUSIONS

In summary, the use of SWV to study pyrene-LPEI/MoFe enzymatic electrode films has enabled direct measurement of the P-cluster ($P^{N/ox}$ couple) and FeMoco ($M^{N/R}$) redox potentials (−0.23 ± 0.01 and −0.60 ± 0.01 V, respectively, under low-turnover conditions). Incorporation of nitrogenase reductase (FeP) into pyrene-LPEI films resulted in a distinct shift in the FeMoco redox potential to −0.43 ± 0.02 V (even in the absence of MgATP). In addition, a nearly identical shift in redox potential for FeMoco was observed in the complete absence of H_2 gas, and voltammetric analysis of MoFe in the

DOI: 10.1021/jacs.9b06546
J. Am. Chem. Soc. 2019, 141, 17150−17157

absence of FeP revealed that electrochemically driven catalysis could only be observed when the atmospheric H_2 content was below ~1.8%. Taken together, this may indicate that the shift in potential of FeMoco is the result of an interaction between MoFe and H_2 where binding of FeP prevents this interaction.

Under all experimental conditions studied herein, the redox potential of FeMoco was observed to be more reducing than that of the P-cluster, suggesting a requisite endergonic electron transfer during catalytic turnover of nitrogenase. In the absence of FeP and under a pure N_2 environment, pyrene-LPEI/MoFe films could take advantage of this apparent endergonic step by driving production of NH_3 from N_2 with an applied potential of −0.25 V at pH 7.0 (consistent with electrochemical reduction of P-cluster but not FeMoco).

■ ASSOCIATED CONTENT

Supporting Information

The Supporting Information is available free of charge on the ACS Publications website at DOI: 10.1021/jacs.9b06546.

Materials, experimental procedures, growth of *Azotobacter vinelandii*, purification of nitrogenase proteins, materials synthesis, bioelectrode fabrication, electrochemical methods, ammonia detection and quantification, and investigation of coimmobilized MoFe/FeP (PDF)

■ AUTHOR INFORMATION

Corresponding Authors

*minteer@chem.utah.edu
*lance.seefeldt@usu.edu
*einsle@biochemie.uni-freiburg.de

ORCID

David P. Hickey: 0000-0002-5297-6895
Rong Cai: 0000-0002-2063-8365
Zhi-Yong Yang: 0000-0001-8186-9450
Katharina Grunau: 0000-0002-0555-8455
Oliver Einsle: 0000-0001-8722-2893
Lance C. Seefeldt: 0000-0002-6457-9504
Shelley D. Minteer: 0000-0002-5788-2249

Author Contributions

‖D.P.H. and R.C. contributed equally to this work.

Notes

The authors declare no competing financial interest.

■ ACKNOWLEDGMENTS

This work was supported by the DOE BETcy EFRC (134124-G003970), Deutsche Forschungsgemeinschaft (RTG 1976 and PP 1927 to O.E.), and the European Research Council (grant 310656 to O.E.). NMR data were collected at the D. M. Grant NMR Center at the University of Utah. The authors would like to thank Sarah E. Soss and Peter F. Flynn for help with the NMR experiments, and Ross D. Milton for valuable discussions related to this work.

■ REFERENCES

(1) Coelho, P. S.; Brustad, E. M.; Kannan, A.; Arnold, F. H. Olefin cyclopropanation via carbene transfer catalyzed by engineered cytochrome P450 enzymes. *Science* **2013**, *339*, 307−310.

(2) Zhang, R. K.; Chen, K.; Huang, X.; Wohlschlager, L.; Renata, H.; Arnold, F. H. Enzymatic assembly of carbon-carbon bonds via iron-catalysed sp^3 C-H functionalization. *Nature* **2019**, *565*, 67.

(3) Bulen, W.; LeComte, J. The nitrogenase system from Azotobacter: two-enzyme requirement for N_2 reduction, ATP-dependent H_2 evolution, and ATP hydrolysis. *Proc. Natl. Acad. Sci. U. S. A.* **1966**, *56*, 979.

(4) Chen, J. G.; Crooks, R. M.; Seefeldt, L. C.; Bren, K. L.; Bullock, R. M.; Darensbourg, M. Y.; Holland, P. L.; Hoffman, B.; Janik, M. J.; Jones, A. K.; Kanatzidis, M. G.; King, P.; Lancaster, K. M.; Lymar, S. V.; Pfromm, P.; Schneider, W. F.; Schrock, R. R. Beyond fossil fuel-driven nitrogen transformations. *Science* **2018**, *360*, No. eaar6611.

(5) Can, M.; Armstrong, F. A.; Ragsdale, S. W. Structure, function, and mechanism of the nickel metalloenzymes, CO dehydrogenase, and acetyl-CoA synthase. *Chem. Rev.* **2014**, *114*, 4149−4174.

(6) Hammes-Schiffer, S.; Klinman, J. Emerging concepts about the role of protein motion in enzyme catalysis. *Acc. Chem. Res.* **2015**, *48*, 899−899.

(7) Armstrong, F. A.; Hill, H. A. O.; Walton, N. J. Direct electrochemistry of redox proteins. *Acc. Chem. Res.* **1988**, *21*, 407−413.

(8) Hoffman, B. M.; Lukoyanov, D.; Yang, Z.-Y.; Dean, D. R.; Seefeldt, L. C. Mechanism of nitrogen fixation by nitrogenase: the next stage. *Chem. Rev.* **2014**, *114*, 4041−4062.

(9) Hu, Y.; Ribbe, M. W. Nitrogenase and homologs. *JBIC, J. Biol. Inorg. Chem.* **2015**, *20*, 435−445.

(10) Lee, C. C.; Hu, Y.; Ribbe, M. W. Vanadium nitrogenase reduces CO. *Science* **2010**, *329*, 642−642.

(11) Yang, Z.-Y.; Moure, V. R.; Dean, D. R.; Seefeldt, L. C. Carbon dioxide reduction to methane and coupling with acetylene to form propylene catalyzed by remodeled nitrogenase. *Proc. Natl. Acad. Sci. U. S. A.* **2012**, *109*, 19644−19648.

(12) Rebelein, J. G.; Hu, Y.; Ribbe, M. W. Differential reduction of CO_2 by molybdenum and vanadium nitrogenases. *Angew. Chem., Int. Ed.* **2014**, *53*, 11543−11546.

(13) Chan, M.; Kim, J.; Rees, D. The nitrogenaseFeMo-cofactor and P-cluster pair: 2.2 Å resolution structures. *Science* **1993**, *260*, 792−794.

(14) Spatzal, T.; Aksoyoglu, M.; Zhang, L.; Andrade, S. L.; Schleicher, E.; Weber, S.; Rees, D. C.; Einsle, O. Evidence for interstitial carbon in nitrogenaseFeMo cofactor. *Science* **2011**, *334*, 940−940.

(15) Einsle, O.; Tezcan, F. A.; Andrade, S. L. A.; Schmid, B.; Yoshida, M.; Howard, J. B.; Rees, D. C. Nitrogenase MoFe-protein at 1.16 Å resolution: acentral ligand in the FeMo-cofactor. *Science* **2002**, *297*, 1696−1700.

(16) Hageman, R. V.; Burris, R. H. Nitrogenase and nitrogenase reductase associate and dissociate with each catalytic cycle. *Proc. Natl. Acad. Sci. U. S. A.* **1978**, *75*, 2699−2702.

(17) Howard, J. B.; Rees, D. C. Structural basis of biological nitrogen fixation. *Chem. Rev.* **1996**, *96*, 2965−2982.

(18) Lanzilotta, W. N.; Christiansen, J.; Dean, D. R.; Seefeldt, L. C. Evidence for coupled electron and proton transfer in the [8Fe-7S] cluster of nitrogenase. *Biochemistry* **1998**, *37*, 11376−11384.

(19) Seefeldt, L. C.; Hoffman, B. M.; Dean, D. R. Mechanism of Mo-dependent nitrogenase. *Annu. Rev. Biochem.* **2009**, *78*, 701−722.

(20) May, H.; Dean, D.; Newton, W. E. Altered nitrogenaseMoFe proteins from Azotobactervinelandii. Analysis of MoFe proteins having amino acid substitutions for the conserved cysteine residues within the β-subunit. *Biochem. J.* **1991**, *277*, 457−464.

(21) Kent, H. M.; Ioannidis, I.; Gormal, C.; Smith, B. E.; Buck, M. Site-directed mutagenesis of the Klebsiella pneumoniae nitrogenase. Effects of modifying conserved cysteine residues in the α-and β-subunits. *Biochem. J.* **1989**, *264*, 257−264.

(22) Lukoyanov, D.; Khadka, N.; Yang, Z.-Y.; Dean, D. R.; Seefeldt, L. C.; Hoffman, B. M. Reductive elimination of H_2 activates nitrogenase to reduce the N≡N triple bond: characterization of the E4(4H) Janus intermediate in wild-type enzyme. *J. Am. Chem. Soc.* **2016**, *138*, 10674−10683.

(23) Rohde, M.; Sippel, D.; Trncik, C.; Andrade, S. L. A.; Einsle, O. The critical E4 state of nitrogenase catalysis. *Biochemistry* **2018**, *57*, 5497−5504.

DOI: 10.1021/jacs.9b06546
J. Am. Chem. Soc. 2019, 141, 17150−17157

(24) Thorneley, R. N.; Lowe, D. The mechanism of Klebsiella pneumoniae nitrogenase action. Pre-steady-state kinetics of an enzyme-bound intermediate in N_2 reduction and of NH_3 formation. *Biochem. J.* **1984**, *224*, 887−894.
(25) Lowe, D.; Thorneley, R. N. The mechanism of Klebsiella pneumoniae nitrogenase action. The determination of rate constants required for the simulation of the kinetics of N_2 reduction and H_2 evolution. *Biochem. J.* **1984**, *224*, 895−901.
(26) Hickey, D. P.; Lim, K.; Cai, R.; Patterson, A. R.; Yuan, M.; Sahin, S.; Abdellaoui, S.; Minteer, S. D. Pyrene hydrogel for promoting direct bioelectrochemistry: ATP-independent electroenzymatic reduction of N_2. *Chem. Sci.* **2018**, *9*, 5172−5177.
(27) Roth, L. E.; Nguyen, J. C.; Tezcan, F. A. ATP- and iron-protein-independent activation of nitrogenase catalysis by light. *J. Am. Chem. Soc.* **2010**, *132* (39), 13672−13674.
(28) Brown, K. A.; Harris, D. F.; Wilker, M. B.; Rasmussen, A.; Khadka, N.; Hamby, H.; Keable, S.; Dukovic, G.; Peters, J. W.; Seefeldt, L. C.; King, P. W. Light-driven dinitrogen reduction catalyzed by a CdS: nitrogenaseMoFe protein biohybrid. *Science* **2016**, *352*, 448−450.
(29) Milton, R. D.; Abdellaoui, S.; Khadka, N.; Dean, D. R.; Leech, D.; Seefeldt, L. C.; Minteer, S. D. Nitrogenase bioelectrocatalysis: heterogeneous ammonia and hydrogen production by MoFe protein. *Energy Environ. Sci.* **2016**, *9*, 2550−2554.
(30) Milton, R. D.; Cai, R.; Abdellaoui, S.; Leech, D.; De Lacey, A. L.; Pita, M.; Minteer, S. D. Bioelectrochemical Haber-Bosch process: An ammonia-producing H_2/N_2 fuel cell. *Angew. Chem., Int. Ed.* **2017**, *56*, 2680−2683.
(31) Cai, R.; Milton, R. D.; Abdellaoui, S.; Park, T.; Patel, J.; Alkotaini, B.; Minteer, S. D. Electroenzymatic C-C bond formation from CO_2. *J. Am. Chem. Soc.* **2018**, *140*, 5041−5044.
(32) Roth, L. E.; Tezcan, F. A. ATP-Uncoupled, Six-electron photoreduction of hydrogen cyanide to methane by the molybdenum-iron protein. *J. Am. Chem. Soc.* **2012**, *134* (20), 8416−8419.
(33) Pierik, A. J.; Wassink, H.; Haaker, H.; Hagen, W. R. Redox properties and EPR spectroscopy of the P clusters of AzotobactervinelandiiMoFe protein. *Eur. J. Biochem.* **1993**, *212*, 51−61.
(34) Schultz, F. A.; Gheller, S. F.; Burgess, B. K.; Lough, S.; Newton, W. E. Electrochemical characterization of the iron-molybdenum cofactor from Azotobactervinelandiinitrogenase. *J. Am. Chem. Soc.* **1985**, *107*, 5364−5368.
(35) Watt, G. D.; Burns, A.; Lough, S.; Tennent, D. L. Redox and spectroscopic properties of oxidized MoFe protein from Azotobactervinelandii. *Biochemistry* **1980**, *19*, 4926−4932.
(36) Imperial, J.; Shah, V. K.; Ugalde, R. A.; Ludden, P. W.; Brill, W. J. Iron-molybdenum cofactor synthesis in AzotobactervinelandiiNif-mutants. *J. Bacteriol.* **1987**, *169*, 1784−1786.
(37) Paustian, T. D.; Shah, V. K.; Roberts, G. P. Apodinitrogenase: purification, association with a 20-kilodalton protein, and activation by the iron-molybdenum cofactor in the absence of dinitrogenase-reductase. *Biochemistry* **1990**, *29*, 3515−3522.
(38) Rees, J. A.; Bjornsson, R.; Schlesier, J.; Sippel, D.; Einsle, O.; DeBeer, S. The Fe-V cofactor of vanadium nitrogenase contains an interstitial carbon atom. *Angew. Chem., Int. Ed.* **2015**, *54*, 13249−13252.
(39) Sippel, D.; Einsle, O. The structure of vanadium nitrogenase reveals an unusual bridging ligand. *Nat. Chem. Biol.* **2017**, *13*, 956.
(40) Eady, R. R. Structure-function relationships of alternative nitrogenases. *Chem. Rev.* **1996**, *96*, 3013−3030.
(41) Smith, B. E.; Eady, R. R. Metalloclusters of the nitrogenases. In *EJB Reviews*; Springer: Berlin/Heidelberg, 1993; pp 79−93.
(42) Lovell, T.; Torres, R. A.; Han, W.-G.; Liu, T.; Case, D. A.; Noodleman, L. Metal substitution in the active site of nitrogenase MFe7S9 (M = Mo^{4+}, V^{3+}, Fe^{3+}). *Inorg. Chem.* **2002**, *41*, 5744−5753.
(43) Chan, J. M.; Christiansen, J.; Dean, D. R.; Seefeldt, L. C. Spectroscopic evidence for changes in the redox state of the nitrogenase P-cluster during turnover. *Biochemistry* **1999**, *38*, 5779−5785.
(44) Kim, C.-H.; Newton, W. E.; Dean, D. R. Role of the MoFeprotein i-subunit histidine-195 residue in FeMo-cofactor binding and nitrogenasecatalysis. *Biochemistry* **1995**, *34*, 2798−2808.
(45) Burgess, B. K.; Lowe, D. J. Mechanism of molybdenum nitrogenase. *Chem. Rev.* **1996**, *96*, 2983−3012.
(46) Page, C. C.; Moser, C. C.; Chen, X.; Dutton, P. L. Natural engineering principles of electron tunnelling in biological oxidation-reduction. *Nature* **1999**, *402*, 47−52.
(47) Lanzilotta, W. N.; Parker, V. D.; Seefeldt, L. C. Electron transfer in nitrogenase analyzed by Marcus theory: evidence for gating by MgATP. *Biochemistry* **1998**, *37*, 399−407.
(48) Davidson, V. L. Chemically gated electron transfer. A means of accelerating and regulating rates of biological electron transfer. *Biochemistry* **2002**, *41*, 14633−14636.
(49) Kurnikov, I. V.; Charnley, A. K.; Beratan, D. N. From ATP to electron transfer: electrostatics and free-energy transduction in nitrogenase. *J. Phys. Chem. B* **2001**, *105* (23), 5359−5367.
(50) Spee, J. H.; Arendsen, A. F.; Wassink, H.; Marritt, S. J.; Hagen, W. R.; Haaker, H. Redox properties and electron paramagnetic resonance spectroscopy of the transition state complex of Azotobactervinelandiinitrogenase. *FEBS Lett.* **1998**, *432*, 55−58.
(51) Lanzilotta, W. N.; Fisher, K.; Seefeldt, L. C. Evidence for electron transfer-dependent formation of a nitrogenase iron protein-molybdenum-iron protein tight complex therole ofaspartate-39. *J. Biol. Chem.* **1997**, *272*, 4157−4165.
(52) Yang, Z.-Y.; Ledbetter, R.; Shaw, S.; Pence, N.; Tokmina-Lukaszewska, M.; Eilers, B.; Guo, Q.; Pokhrel, N.; Cash, V. L.; Dean, D. R.; Antony, E.; Bothner, B.; Peters, J. W.; Seefeldt, L. C. Evidence that the Pi release event is the rate-limiting step in the nitrogenase catalytic cycle. *Biochemistry* **2016**, *55*, 3625−3635.
(53) Guth, J. H.; Burris, R. H. Inhibition of nitrogenase-catalyzed ammonia formation by hydrogen. *Biochemistry* **1983**, *22*, 5111−5122.
(54) Sargsyan, H.; Gabrielyan, L.; Trchounian, A. Concentration-dependent effects of metronidazole, inhibiting nitrogenase, on hydrogen photoproduction and proton-translocating ATPase activity of Rhodobactersphaeroides. *Int. J. Hydrogen Energy* **2014**, *39*, 100−106.
(55) Dance, I. The hydrogen chemistry of the FeMo-co active site of nitrogenase. *J. Am. Chem. Soc.* **2005**, *127*, 10925−10942.
(56) Durrant, M. C. An atomic-level mechanism for molybdenum nitrogenase. Part 2. proton reduction, inhibition of dinitrogen reduction by dihydrogen, and the HD formation reaction. *Biochemistry* **2002**, *41*, 13946−13955.
(57) Burris, R. H.; Wilson, P. W. Characteristics of the nitrogen-fixing enzyme system in nostocmuscorum. *Bot. Gaz.* **1946**, *108*, 254−262.
(58) Lee, H.-I.; Cameron, L. M.; Hales, B. J.; Hoffman, B. M. CO Binding to the FeMocofactor of CO-inhibited nitrogenase: ^{13}CO and ^{1}H Q-Band ENDOR investigation. *J. Am. Chem. Soc.* **1997**, *119*, 10121−10126.
(59) Smits, R. G.; Koper, G. J. M.; Mandel, M. The influence of nearest- and next-nearest-neighbor interactions on the potentiometric titration of linear poly(ethylenimine). *J. Phys. Chem.* **1993**, *97*, 5745−5751.
(60) Davydov, R.; Khadka, N.; Yang, Z. Y.; Fielding, A. J.; Lukoyanov, D.; Dean, D. R.; Seefeldt, L. C.; Hoffman, B. M. Exploring electron/proton transfer and conformational changes in the nitrogenaseMoFeprotein and FeMo-cofactor through cryoreduction/EPR measurements. *Isr. J. Chem.* **2016**, *56*, 841−851.
(61) Lanzilotta, W. N.; Seefeldt, L. C. Changes in the midpoint potentials of the nitrogenase metal centers as a result of iron protein-molybdenum-iron protein complex formation. *Biochemistry* **1997**, *36*, 12976−12983.

DOI: 10.1021/jacs.9b06546
J. Am. Chem. Soc. 2019, 141, 17150−17157